High pressure phase transitions and hydrogen-bond symmetry in ice polymorphs

Kenneth S. Schweizer and Frank H. Stillinger
Bell Laboratories, Murray Hill, New Jersey 07974

(Received 16 August 1983; accepted 25 October 1983)

A recently developed ground state variational wave function theory of hydrogen-bonded crystals is employed to investigate the high pressure behavior of several ice polymorphs. The theory accurately accounts for short and long range proton correlations and quantum mechanical tunneling, all of which are important in the high pressure regime. Attention is focused on pressure induced order–disorder phase transitions and hydrogen-bond symmetrization for the ices VII, VIII, and Ic. We find a strongly first order transition (driven by proton tunneling) at approximately 330 kbar from the antiferroelectrically ordered ice VIII phase to a highly ionized form of proton disordered ice VII. Despite the large degree of ionization, significant short range proton order remains at the transition as indicated by the bimodality of the proton charge density along the bond. The crossover to a unimodal situation, i.e., hydrogen-bond symmetrization, is predicted to occur at 450 kbar. The effects of deuterium isotope substitution on these phenomena are also studied. Calculations for the lower density cubic form of ice indicate that it may be possible to observe symmetrical hydrogen bonds in this material at a significantly lower pressure than those required for the dense ices.

I. INTRODUCTION

Recent development of the diamond anvil pressure cell technique has opened up new vistas in the area of high pressure research.[1] The accessibility of megabar pressures under controlled conditions allows the study of a range of fascinating new phenomena in a variety of materials. Very recently, Raman and x-ray techniques were applied[2] in a study of the high pressure properties of the proton disordered ice VII. A major goal of that work was the search for symmetrical hydrogen bonds at very high pressure. Such a situation corresponds to a radical change in the bonding of protons in the ice crystal. At low pressures, protons exhibit a very strong degree of short range order owing to their overwhelming propensity to form intact water molecules. However, as the oxygen atoms of the ice lattice are pushed closer together by applying pressure, the picture of ice as a molecular crystal begins to break down. At some specific very high pressure, one expects to enter the regime where the proton charge density along the bond exhibits a single maximum at precisely the bond midpoint. Such a situation is usually referred to as a symmetrical hydrogen bond. Clearly, the strong short range proton order has been destroyed at this point and ice can no longer be described as a molecular crystal but rather something more akin to a covalent or ionic solid. Such a "transition" is not expected to be a true thermodynamic phase change but rather a more gradual phenomenon describing the "crossover" from a molecular picture to one where virtually all short range proton order has disappeared. This crossover phenomenon is directly observable via neutron diffraction and indirectly by the dramatic changes expected to occur in the vibrational dynamics associated with proton motions. In particular, the description of proton motions as perturbed molecular oscillators must be replaced by an anharmonic phonon picture.

The crossover in the nature of the dynamical excitations of ferroelectric materials near structural phase transitions has been of considerable theoretical and experimental interest recently.[3] In particular, the appearance above the transition temperature of an intense central peak in dynamic light scattering experiments has been interpreted as a signature of the crossover phenomenon. It is thought to represent the onset of short range order or cluster formation that acts as a precursor for the low temperature long range ordered phase. Similar intense central peak phenomena have recently been observed for hexagonal ice at atmospheric pressure.[4] The microscopic origin of this peak is not understood at present, but its evolution under pressure is certainly an interesting question which may be related to the expected destruction of short range proton order as one approaches the hydrogen-bond symmetrization regime. Recent workers have speculated[4] that the central peak is intimately related to defects in the ice crystal. If this is true then pressure measurements may be very helpful in unraveling the mechanism of this phenomenon since the orientational (Bjerrum) and ionic defects behave very differently as a function of pressure.

Another interesting phenomenon becomes possible at very high pressures if one studies a crystal that exhibits long range proton order at relatively low pressures, e.g., the antiferroelectric ice VIII. Increasing pressure deforms the bond potential that a proton experiences in such a way as to give rise to a tunnel splitting of the ground vibrational level. This introduces quantum fluctuations into the system corresponding to proton tunneling from one side of the bond to the other. Such fluctuations tend to destroy the long range proton ordered state and eventually one expects the competition between proton tunneling and proton–proton interactons to lead to a phase transition of the order–disorder type. Such a phase change is observable via a variety of experimen-

 0021-9606/84/031230-11$02.10

tal methods (e.g., dielectric constant, polarization hysteresis loops, calorimetry). A related question is whether the phase transition occurs before (i.e., at lower pressure) or after the hydrogen bond symmetrizes.

We have previously attempted to address these questions theoretically for several ice polymorphs[5] (we hereafter refer to that paper as I). Simple mean field theory and soft mode calculations were employed and our tentative conclusion was that pressures of the order of 0.5–1 Mbar were needed to observe the order–disorder phase transition and hydrogen-bond symmetrization. The picture of the phase transition that emerged from the simple treatment was a continuous (second order) phase change driven by the appearance of a large number of ions in the crystal due to proton tunneling. In particular, there was an ionization catastrophe in the sense that the maximum number of ions that can be present in ice appears at the transition point. At higher pressures the ice was proton disordered, and is describable in terms of independent protons coherently tunneling back and forth.

The basic prediction of mean field theory is a pressure induced phase transition from a proton ordered to a proton disordered state. This is certainly qualitatively correct. However, mean field theory is not quantitatively reliable and its detailed qualitative predictions of a continuous phase change and complete ionization catastrophe as the mechanism of the symmetry breaking cannot be trusted. Indeed, because the pressures needed to observe the transition are expected to be so high, a quantitatively reliable prediction of the transition pressure is a serious experimental question. These considerations have led us very recently to develop a much more detailed theory which simultaneously addresses the questions of short range and long range proton correlations and the quantum tunneling aspect[6] (we hereafter refer to that paper as II). We have argued in paper II that such a theory should be quite accurate for the three dimensional materials of interest.

The purpose of the present paper is to apply our recently developed theory to examine quantitatively the high pressure behavior of several ice polymorphs. We shall be concerned primarily with the dense ices VII and VIII. Cubic ice I will be briefly considered. The questions and phenomena addressed for ice in this paper are also relevant to a variety of more well studied hydrogen-bonded ferroelectric crystals. The application of the theory to these materials is discussed elsewhere.[7]

The remainder of the paper is structured as follows. In Sec. II we briefly discuss the theory and summarize the relevant formulas. Calculations and predictions for the high pressure ice polymorphs of interest are presented in Sec. III. The effect of isotope substitution and the detailed qualitative physical picture of the quantum-fluctuation-driven transition are discussed. The paper concludes with a discussion of the significance of our work and future directions of research.

II. THEORY

The present section is devoted to a brief outline of the theory developed in paper II. Only the zero temperature ground state problem was addressed in II. There are three reasons for such a restricted view. First, there is the obvious theoretical simplification obtained by neglecting excited states. Second, the low temperature regime is of fundamental interest because thermal fluctuations will be largely frozen out thereby enabling one to study more directly the purely quantum aspect of the proton tunneling driven high pressure phenomena. Finally, even at the high pressures of interest, ion formation energies are still large enough that the activated thermal mechanism for their creation appears to be a much less efficient process as compared to the purely quantum mechanical state mixing mechanism, even at relatively high temperatures. This statement will be made more precise in Sec. III where calculations are presented to support this conclusion.

A. Model Hamiltonian

We begin by considering the Hamiltonian adopted to describe the interacting protons in ice. There are three basic considerations. Two of these involve a detailed description of the energetics associated with the different (localized) proton configurations in the crystal. The first consideration is that protons prefer to be arranged in such a fashion as to obey the Bernal–Fowler–Pauling ice rules,[8] i.e., they form intact water molecules. This tendency arises microscopically from short range (four-body) proton–proton interactions between the four protons surrounding a particular oxygen. We therefore introduce the positive energies ϵ_1 and ϵ_2 (a neutral water molecule is taken to correspond to zero energy) needed to form a singly charged ion (H_3O^+ and OH^-) and a doubly charged ion (H_4O^{++} and O^{--}), respectively. The second consideration addresses the fact that there are longer ranged residual two-body interactions between protons, primarily of dipole character. It is these interactions that lift the degeneracy of the different neutral water molecule configurations in the crystal. In particular, one can identify[5] a single neutral water molecule configuration (and its symmetry-related partners) that has the lowest classical potential energy, $-2NJ$, where $2N$ is the number of protons in the crystal. For this lowest energy, long range proton ordered state, each proton has a unique side of the bond it prefers to inhabit. These two considerations suggest a classification scheme based on the number of oxygens in ice of a particular "type" or "state." For each configuration of protons, every oxygen is classified by: (1) its charge state (ionicity = the number of protons "belonging" to it), and (2) the position of each proton, either "right" (r) or "wrong" (w) as defined by the lowest energy long ranged proton ordered configuration. The former criterion introduces the order parameters $\{N_\alpha\}$ which represent the number of oxygens in the crystal of type α. Several examples are shown in Fig. 1. The latter criterion introduces an order parameter x that measures the degree of long range proton order. It is defined such that $2Nx$ is the number of protons in the crystal that are in the wrong position. Detailed analysis[6] allows a description in terms of five independent order parameters or oxygen types with the resulting potential energy per proton:

$$V/2N = \epsilon_1(x_r + x_w) + \epsilon_2 x_0 - J(1-2x)^2, \tag{2.1}$$

where the oxygen type fractions $x_\alpha = N_\alpha/N$ have been in-

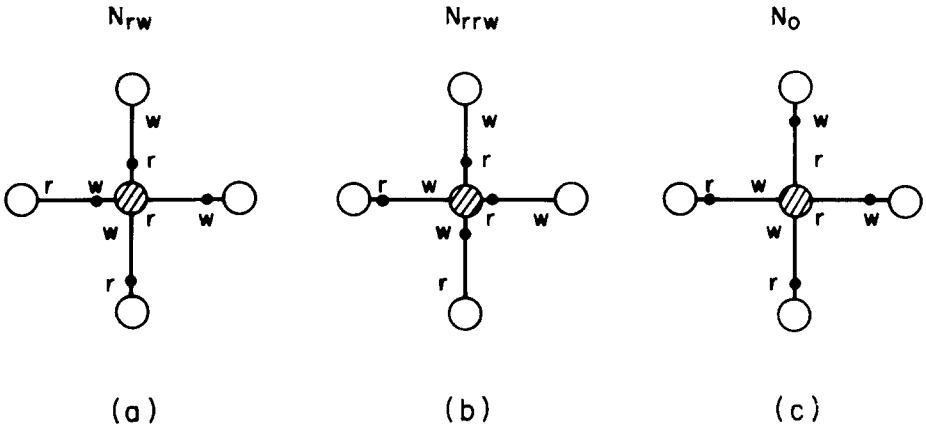

FIG. 1. Four coordinated vertex with the two possible proton positions along each bond labeled as right (r) or wrong (w). Three different proton configurations around the central vertex are displayed along with their corresponding notational designation.

troduced and where x_r and x_w can be expressed in terms of the five independent order parameters, x, x_0, x_{rr}, x_{rw} and x_{ww}:

$$x_r = (x - \tfrac{1}{2}) + \tfrac{1}{4}(x_{rr} - x_{rw} - 3x_{ww} - 2x_0), \tag{2.2}$$

$$x_w = (\tfrac{3}{4} - x) + \tfrac{1}{4}(x_{ww} - x_{rw} - 3x_{rr} - 2x_0). \tag{2.3}$$

The long range residual dipole interaction in Eq. (2.1) has been treated at a mean field or infinite range level.

The final consideration is quantization of proton motion. We adopt a two-state model corresponding to the pair of resonance-split ground vibrational states. For concreteness we employ a double Morse potential model (see Appendix for details) for the single bond proton motion (see Fig. 2). The one-body Schrödinger equation can be solved for the two lowest energy states $\Phi_0(r)$ and $\Phi_1(r)$ and their corresponding energies E_0 and E_1, respectively. Symmetric and antisymmetric linear combinations of these states yield orbitals $\Phi_\pm(r)$ that are localized on one side of the bond or the other. By working in this representation of localized or wave packet states one can identify the proton as being on either the right or wrong side of the bond. The single bond Hamiltonian matrix element that couples these two localized states is referred to as the tunnel splitting K and is given by $2K \equiv E_1 - E_0$. This two-state description is mathematically expressible in terms of the usual Pauli spin oprators, with kinetic energy given by

$$T = -K\sum_{i=1}^{2N} S_i^x. \tag{2.4}$$

The full many-body Hamiltonian is taken to be the sum of Eqs. (2.1) and (2.4):

$$\mathsf{H} = T + V. \tag{2.5}$$

The model introduces four characteristic energies: K, ϵ_1, ϵ_2, J describing the quantum tunneling, short range, and long range proton–proton interactions, respectively. The parameters are both crystal-structure and pressure dependent.

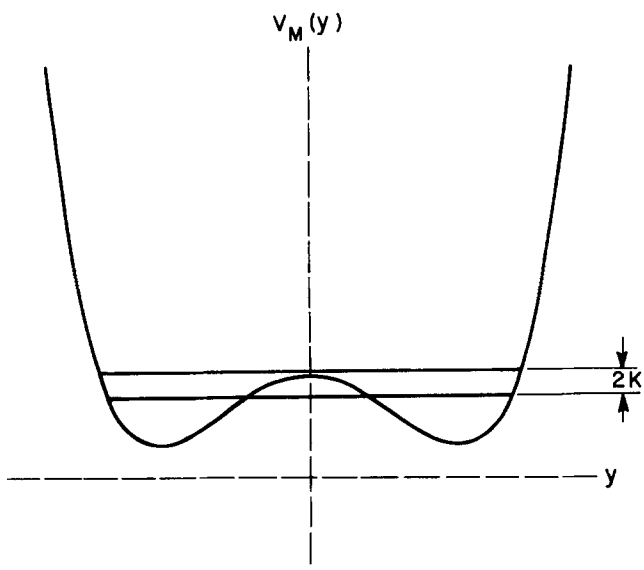

FIG. 2. Typical form of the double Morse potential in the high pressure regime. The abscissa y is the deviation of the proton position from the bond midpoint. The pair of tunnel-split ground vibrational levels are separated by an energy 2 K.

B. Ground state wave function

The zero temperature properties of the Hamiltonian (2.5) are obtained by constructing a theory for the ground state wave function. A formally exact expression for the ground state can be written as a linear combination of the orthonormal Hartree orbitals:

$$\Psi = \sum_{\{S_k\}} A(\{S_k\}) \prod_{j=1}^{2N} \chi_j(S_j;\{S_k\}), \tag{2.6}$$

where $\{S_k\}$ denotes a particular configuration of all the protons (S_k is the eigenvalue of the z-component Pauli spin operator and can assume the values ± 1 corresponding to the two possible proton positions in each bond) and $\chi_j(S_j;\{S_k\})$ indicates which side of the bond proton j is on for the configuration $\{S_k\}$. Further progress requires the selection of a trial wave function in which the dependence of the amplitudes $A(\{S_k\})$ on the specific proton configuration $\{S_k\}$ has been simplified. The fundamental approximation introduced in paper II was the adoption of a trial wave function of the form:

$$\Psi_t \equiv \sum_{\{N_\alpha,x\}} A(\{N_\alpha\},x) \sum_{\{S_k\}\in\{N_\alpha,x\}} \prod_{j=1}^{2N} \chi_j(S_j;\{S_k\}). \tag{2.7}$$

The physical content of this approximation is that all proton configurations with the same set of order parameters or oxy-

types, $\{N_\alpha, x\}$, occur with equal probability in the ground state. As a consequence, for a fixed set of $\{N_\alpha, x\}$ the real-space proton positions are random subject only to the global oxygen type number constraints and geometrical exclusion constraints. Detailed analysis[6] allows one to derive an explicit expression for the trial ground state energy in terms of the five independent variational parameters:

$$E/2NK \equiv T/2NK + V/2NK, \tag{2.8}$$

$$V/2NK \equiv (\epsilon_1/K)(x_r + x_w) + (\epsilon_2/K)x_0 - (J/K)(1-2x)^2 \tag{2.9}$$

$$\begin{aligned} T/2NK \equiv [x(1-x)]^{-1/2}\{&2x_0(x_r x_w)^{1/2} + x_0(x_r + x_w) + 2x_{rw}(x_r x_w)^{1/2} + x_r[2(x_0 x_{rw})^{1/2} + 2(x_{rw}x_{rr})^{1/2} \\ &+ 2(x_0 x_{rr})^{1/2} + x_{rr} + x_{rw}] + x_w[2(x_0 x_{rw})^{1/2} + 2(x_{rw}x_{ww})^{1/2} + 2(x_0 x_{ww})^{1/2} + x_{ww} + x_{rw}] \\ &+ 4(x_0 x_r x_w x_{rw})^{1/2} + 2(x_0 x_r x_w x_{rr})^{1/2} + 2(x_0 x_r x_w x_{ww})^{1/2} + 2(x_r x_w x_{rw} x_{ww})^{1/2} \\ &+ 2(x_r x_w x_{rw} x_{rr})^{1/2} + 2(x_r x_w x_{rr} x_{ww})^{1/2}\}, \end{aligned} \tag{2.10}$$

where $x_\alpha \equiv \langle \Psi_t | N_\alpha | \Psi_t \rangle / N$, and x_r and x_w are given by Eqs. (2.2) and (2.3). The five parameters x_α are determined by energy minimization

$$\frac{\partial E}{\partial x_\alpha} = 0. \tag{2.11}$$

The structural quantity relevant to the hydrogen-bond symmetrization question is the proton density along a bond

$$\rho(r) \equiv \langle \Psi_t | \delta(r - r_1) | \Psi_t \rangle. \tag{2.12}$$

Within the context of the present theory, one can derive the explicit result

$$\rho(r) = \tfrac{1}{2}\{[x^{1/2} + (1-x)^{1/2}]\Phi_0(r) + [x^{1/2} - (1-x)^{1/2}]\Phi_1(r)\}^2 + \tfrac{1}{2}\{\langle S^x \rangle - 2[x(1-x)]^{1/2}\}[\Phi_0(r) + \Phi_1(r)][\Phi_0(r) - \Phi_1(r)]. \tag{2.13}$$

As before, Φ_0 and Φ_1 are the ground and first excited states for the single bond (double Morse potential) Schrödinger equation and $\langle S^x \rangle = T/2NK$ in Eq. (2.10). It is important to note that even in the proton disordered phase ($x \equiv \frac{1}{2}$), $\rho(r)$ is not the independent proton density (i.e., ground state $|\Phi_0(r)|^2$). In general, there is a condensed-phase-induced component, given by the second term in Eq. (2.13), due to short range proton correlations that tend to suppress tunneling.

III. APPLICATIONS

A. Hamiltonian parameters

To apply our theory to real materials we must determine the values of the interaction parameters ($K, \epsilon_1, \epsilon_2, J$) and their dependence on pressure. The general philosophy adopted has been to employ all the relevant experimental information that is available to determine the parameter values at low pressure. The change in these values with pressure is calculated with the aid of specific models.

1. Bond potential

A bond potential of the double Morse form has been employed. The details of the potential are discussed in the Appendix. The important feature is its dependence on four parameters: $r_{OH}, R_{OO}, V_{OH}, \alpha_{OH}$. We follow Holzapfel[9] and fix these potential parameters from known information. In particular the OH covalent bond length (r_{OH}), oxygen–oxygen separation (R_{OO}), bond dissociation energy (V_{OH}), ionic activation energy (E_A), and OH stretch zero point energy ($\hbar\omega_0/2$) at atmospheric pressure are employed. These values are summarized in Table I along with the determined potential parameters. As demonstrated by Holzapfel,[9] the resulting Morse potential prediction for the variation of OH covalent bond length with oxygen–oxygen separation $r_{OH}(R_{OO})$ is in good agreement with direct experimental measurements[11] of r_{OH} and R_{OO} for a wide variety of hydrogen-bonded materials. In addition, the model Morse potential changes from bistable to monostable at $R_{OO} \simeq 2.4$ Å. This result is in good agreement with *ab initio* quantum chemical calculations on small water clusters.[12] We therefore expect this bond potential to be reliable over a wide range of pressure. Different ice polymorphs have different values for r_{OH} and R_{OO}, but we assume the ion activation energy, zero point energy, and bond dissociation energy are identical.

We also require the tunneling splitting K of the ground vibrational state as a function of R_{OO} (i.e, pressure). Explicit calculation of this quantity for the double Morse potential is discussed in the Appendix.

TABLE I. Parameters employed for the low pressure situations (atmospheric pressure for ice I and $\simeq$21 kbar for the dense ices). The values were obtained from Ref. 10 unless indicated otherwise.

	Ice VII/VIII	Ice I
r_{OH} (Å)	0.95	1.0
R_{OO} (Å)	2.86	2.76
V_{OH} (kcal/mol)[a]	123	123
E_A (kcal/mol)[b]	13	13
ϵ_∞	2.56	1.70
$\hbar\omega_0/2$(kcal/mol)[c]	5	5
α_{OH} (Å^{-1})[d]	2.8	3.1

[a] Taken to be the sum of the single water molecule bond dissociation energy (118 kcal/mol) and the proton zero point energy.
[b] Reference 9.
[c] The small differences between the proton zero point energy in the dense ices and ice I have been ignored. We have adopted the same value employed in Ref. 9.
[d] Determined by requiring that the barrier separating the two minima of the double Morse bond potential be equal to the sum of the ionic activation energy and the proton zero point energy.

2. Proton interaction energies

The relevant parameters are the singly and doubly charged ion formation energies ϵ_1 and ϵ_2, respectively, and the stabilization energy per proton J of the lowest energy long range proton ordered state. The singly charged ion formation energy has been experimentally measured[10] for hexagonal ice and is found to be 11 ± 1.5 kcal/mol. The corresponding quantity for the dense ices VII and VIII is not available. We therefore estimate the appropriate value by assuming the primary microscopic interaction between protons that determines the energetics is of dipolar form. In this case, all protonic energies scale with the factor f:[5]

$$f \equiv (q^2/\epsilon_\infty)|\langle \Phi_0|r|\Phi_1\rangle|^2/R_{OO}^3. \tag{3.1}$$

Here, q is the effective proton charge, ϵ_∞ the optical dielectric constant, R_{OO} the oxygen separation, and $\langle \Phi_0|r|\Phi_1\rangle$ the dipole matrix element. Hence, we estimate the ionic formation energy for ice VII (and by implication ice VIII) by

$$\epsilon_1(\text{VIII}) = \frac{f(\text{VII})}{f(\text{I})} \cdot 11 \frac{\text{kcal}}{\text{mol}}. \tag{3.2}$$

To implement Eq. (3.2) we employ known structural parameters for the two ices (see the table) and assume q to be the same for the two polymorphs. The resulting estimate is sufficiently close to the hexagonal ice value that in view of the crudeness of our calculation we simply adopt the value of 11 kcal/mol for the dense ices also.

Direct measurement of the doubly charged ion formation energy ϵ_2 are not available. Simple estimates based on the point dipole model yield $\epsilon_2 = 3\epsilon_1$. We expect this to be a lower bound since packing four protons around an oxygen will lead to additional short range overlap repulsive contributions to the energy. We adopt the value $\epsilon_2 = 4\epsilon_1$. Our results are not sensitive to reasonable variations of this quantity.

The long range interaction energy J is fixed by requiring the experimentally determined low pressure (~ 21 kbar) phase transition temperature $T_c = 0\,^\circ\text{C}$ be reproduced by the *classical* finite temperature cluster theory with the parameters ϵ_1 and ϵ_2 chosen as described above. There are slightly different formulations of the classical theory due to many workers.[13–15] We employ the formulas given by Eqs. (3.6)–(3.10) in paper II. Application of this approach yields a very strong first order transition as is observed experimentally. A value of $J = 0.174\ T_c$ is required to reproduce the experimental transition temperature.

The trial ground state energy [Eqs. (2.8)–(2.10)] can be expressed as a function of three dimensionless energy scales: $E(\epsilon_1/J, \epsilon_2/\epsilon_1, K/J)$. For the dense ices VII and VIII one has $\epsilon_1/J = 110$ and $\epsilon_2/\epsilon_1 = 4$. The simplifying assumption that these three energies have a common microscopic origin requires they exhibit the same pressure dependence. Therefore, ϵ_1/J and ϵ_2/ϵ_1 are taken to be pressure *independent*. Pressure dependence enters solely via the parameter K/J. The dependence of K on pressure (or equivalently R_{OO}) is calculated directly from the Morse bond potential model, while J is assumed to vary with pressure as the factor f in Eq. (3.1) with q^2/ϵ_∞ taken to be oxygen separation independent. Equation of state data is available for the dense ices[2,16] allowing us to compute the pressure corresponding to a given R_{OO}.

B. Ice VIII/VII

The dense ices VII and VIII are composed of a pair of interpenetrating but not interconnecting hydrogen-bonded ice Ic sublattices (see Fig. 3). They are stable only at pressures exceeding roughly 20 kbar. Ice VII has a body centered cubic structure in which each water molecule is eightfold coordinated. It is largely proton disordered over its canonical ice-rule structures. The crystal of ice VIII is tetragonal, corresponding to a slight ($\eta \simeq 0.022$[17] in Fig. 3) distortion of one sublattice with respect to the other. This form is strongly proton ordered in an antiferroelectric fashion corresponding to completely polarized sublattices of water molecules with their molecular dipoles all parallel and antiparallel to the tetragonal distortion axis.[10] At room temperature, ice VII is the stable phase but upon cooling to about 0 °C one encounters a strong first order phase boundary below which ice VIII is stable.

1. Pressure induced order–disorder phase transition

Calculations were performed by numerically solving the five coupled algebraic equations (2.11) with the interaction parameters discussed above. The variation of tunnel splitting and proton–proton interaction energies with oxygen separation is shown in Fig. 4. We find a strong first order phase transition from the ordered ice VIII phase to disordered ice VII at a pressure of 330 kbar ($R_{OO} = 2.523$ Å). The corresponding deuterated crystal undergoes a transition at $R_{OO} \simeq 2.49$ Å or 390 kbar (the only effect of deuteration was assumed to be the mass change and hence decreased tunnel splitting). The pressure dependence of the long range order parameter ($|1 - 2x|$, assumed to be proportional to the sub-

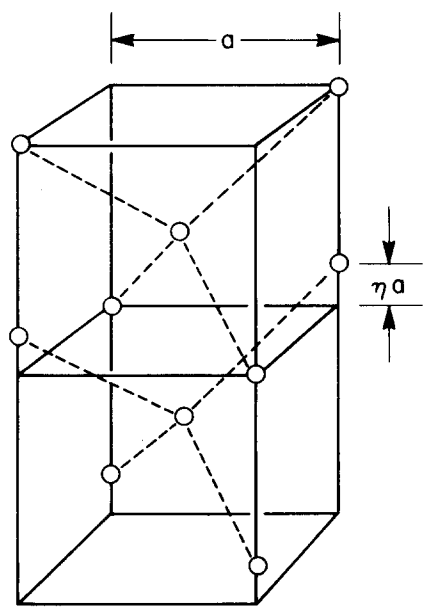

FIG. 3. Oxygen lattice framework for the dense ices. The lattice constant is labeled a, and η is the uniaxial displacement parameter which is zero for ice VII but nonzero for ice VIII.

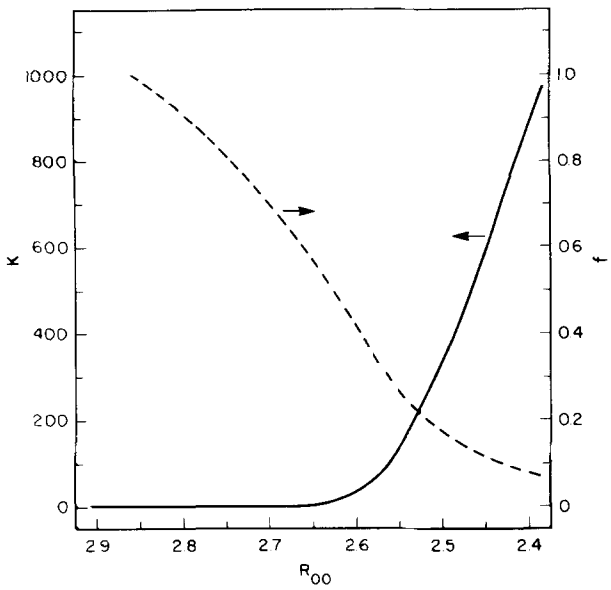

FIG. 4. The solid curve is the tunnel splitting K in cm^{-1} for the dense ices plotted as a function of oxygen separation in angstroms. The dipolar scale factor [see Eq. (3.1)] in arbitrary units is denoted by the dashed curve.

lattice polarization) is shown in Fig. 5. The transition should be directly detectable by dielectric measurements analogous to those employed by Whalley[18] in his pioneering work that led to the discovery of ice VIII.

In an effort to gain a more microscopic picture of the transition, we have calculated the singly charged ion concentration at high pressure. Figure 6 presents our results for the logarithm of the hydronium ion concentration as a function of pressure or oxygen separation. There are several points of interest concerning these results. One is the dramatic increase in ion concentration as the pressure increases. At the

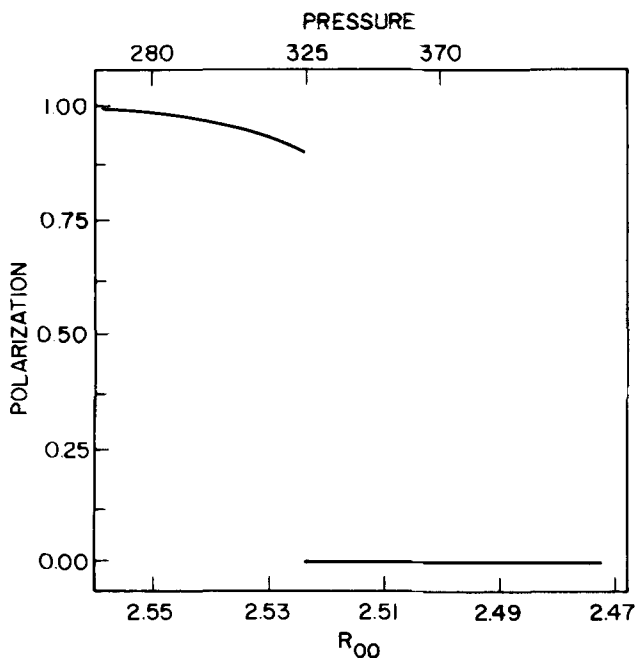

FIG. 5. Sublattice polarization as a function of oxygen separation (angstroms) and pressure (kbar).

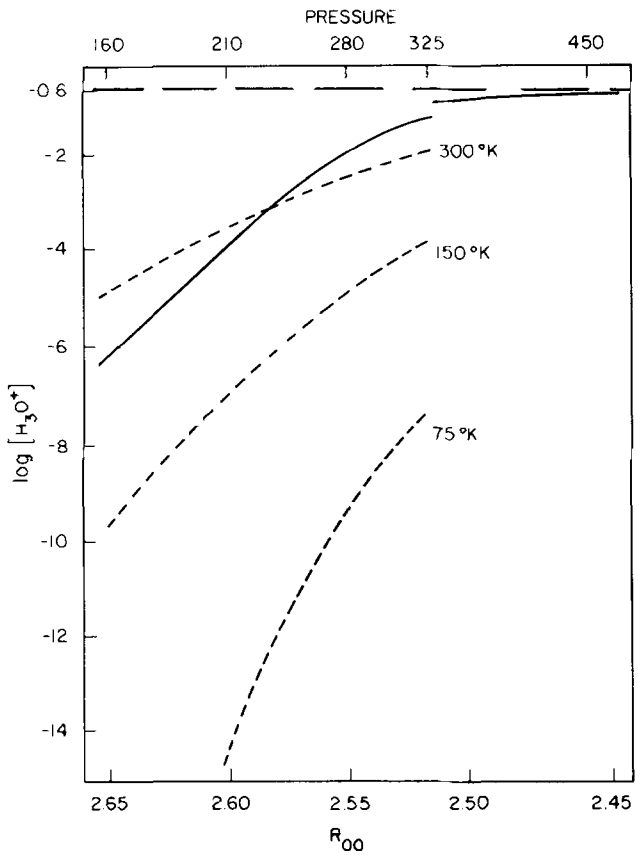

FIG. 6. The solid curve is the ground state theory calculation of the logarithm of the hydronium ion concentration as a function of oxygen separation (angstroms) and pressure (kbar). The horizontal long-dashed line is the asymptotic limit corresponding to a random (entirely uncorrelated) distribution of protons in ice. The short-dashed curves are the classical finite temperature predictions discussed in the text.

transition the crystal is highly ionized, $[H_3O^+] \simeq 0.063$, and there is a discontinuous jump in $[H_3O^+]$ by a factor of approximately 2.1. Nevertheless, one does not have a complete ionization catastrophe as predicted by the simple mean field theory.[5] The protons are not randomly distributed on either side of the bond (this would correspond to $[H_3O^+] = 0.25$) but still prefer to arrange themselves in such a way as to form intact water molecules. Just below the transition the concentration of intact water molecules is approximately 0.87. Consequently, there is still a significant amount of short range proton order at the transition.

In the strongly ordered regime (polarization $\geqslant 0.98$), the dependence of the ion concentration on tunnel splitting is particularly simple:

$$[H_3O^+] \propto K^2. \tag{3.3}$$

Such behavior is expected from first order perturbation theory mixing of ionic configurations into the neutral water molecule ground state. The constant of proportionality is a decreasing function of ϵ_1 and ϵ_2.

It is clear from our calculations that the physical mechanism for destruction of the ordered phase is the dramatic increase in ionic configurations due to quantum mechanical tunneling. Strictly speaking, the theory applies only to the zero temperature case or at best to the very low temperature

regime. The question then arises as to whether our results have any significance at the more readily accessible elevated temperatures, e.g., $75 \leqslant T \leqslant 300$ K. This question can be unambiguously answered only if we can generalize the present theory to finite temperatures. This problem is under study but has not been fully resolved. However, one can gain a qualitative feeling for the importance of thermal fluctuations by asking the following question: If one turns off the quantum tunneling ($K = 0$), how does the *thermally* generated ion concentration increase with pressure? This question can be answered by applying the finite temperature classical cluster theory discussed previously in regard to the determination of the parameter J for the ice VIII/VII transition. The results of such a calculation for three temperatures is shown in Fig. 5. At high pressures, the over-the-barrier thermal fluctuation mechanism for ion creation is clearly insignificant compared with the quantum tunneling process for the 75 and 150 K cases. At 300 K, the classical thermal fluctuation mechanism is important, but near the transition pressure the quantum process again becomes more efficient. The reason for this behavior is that although the ion formation energy decreases with pressure (see Fig. 4), it is still large compared to the thermal energy scale. Therefore, since the classical ion concentration is roughly proportional to $\exp(-\epsilon_1/k_B T)$, this mechanism is still relatively inefficient. These results suggest that thermal fluctuations at finite T may not seriously modify the predictions we have made using the ground state quantum theory. One conclusion that can be emphatically drawn is that finite temperature effects can only destabilize the ordered phase, thereby lowering our predicted transition pressure.

Another interesting question involves the nature of the proton density along a bond at the transition. This has been computed using Eq. (2.13) and the result is displayed in Fig. 7. Because the transition is strongly first order, there is a

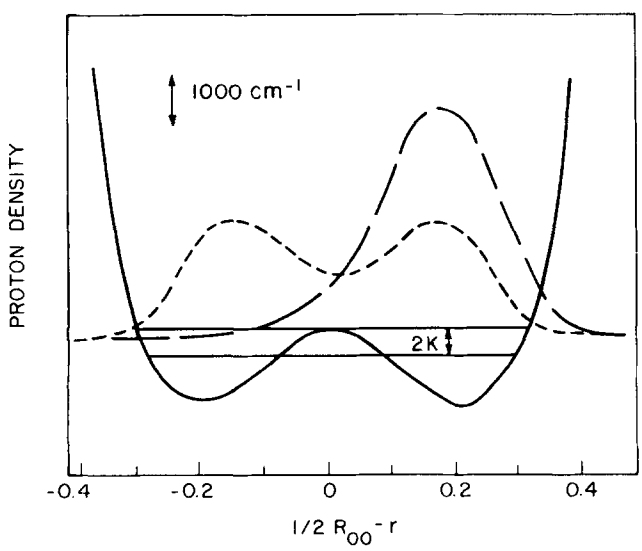

FIG. 7. Normalized proton density along the bond plotted as a function of the displacement (in angstroms) from the bond midpoint. The proton density at a pressure just below (long-dashed curve) and just above (short-dashed curve) the first order phase transition is shown. The single bond Morse potential and the corresponding pair of tunnel-split energy levels are also displayed with the energy scale indicated by the vertical arrow.

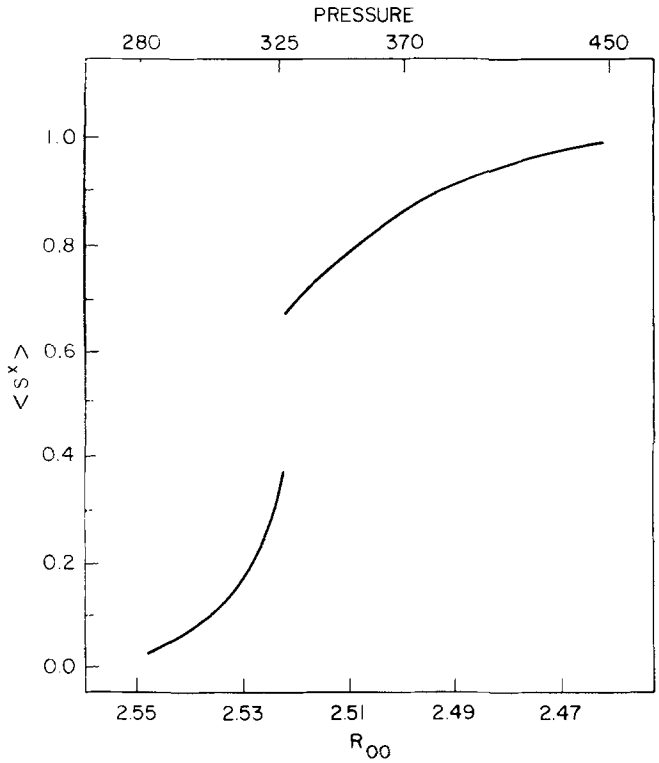

FIG. 8. Ground state average of the kinetic energy or tunneling operator as a function of oxygen separation (angstroms) and pressure (kbar).

dramatic discontinuous expansion of the proton density along the bond at the transition. However, the disordered phase proton density is still strongly bimodal thereby indicating the presence of a significant degree of short range proton order even though the material is highly ionized. Clearly, further compression is required to reach the point where the hydrogen bond becomes symmetrized (unimodal).

Another property related to the proton density along the bond is the average kinetic energy operator $\langle S^x \rangle$ which is a measure of the effective tunnel splitting K_{eff} in the condensed phase.[6] At zero temperature this relationship can be made precise by defining

$$K_{\text{eff}} = K \langle S^x \rangle . \tag{3.4}$$

In general, $\langle S^x \rangle < 1$ due to the localizing influence of the short and long range proton–proton interactions. Figure 8 vividly demonstrates the importance of the short range correlations even above the transition.

2. Hydrogen-bond symmetrization

We now turn to the question of hydrogen-bond symmetrization. Experimentally, one can detect this crossover phenomenon directly by neutron diffraction. These experiments are difficult, however, and recent workers[2] have taken the indirect approach of Raman scattering measurements in the O–H stretching frequency regime. The idea is that as R_{OO} decreases, the O–H bond length r_{OH} stretches and this leads to the well known decrease of the O–H force constant and corresponding shift of the O–H stretching frequency to the red. Eventually, when the proton has moved to the bond center on the average ($r_{OH} = R_{OO}/2$), further compression of R_{OO} will increase the force constant and lead to an in-

crease in frequency of the Raman peak. Therefore, the hydrogen-bond symmetrization point should be detectable as a minimum in the Raman peak position as a function of pressure. Walrafen *et al.*[2] have searched for this phenomenon in ice VII at room temperature up to 320 kbar but found no such minimum. We have applied our theory to this question by calculating the pressure at which the single bond proton density becomes peaked at the bond midpoint. A rigorous equivalence of this criterion for hydrogen-bond symmetrization and the Raman peak minimum is not obvious but on intuitive physical grounds one expects the two criteria to be very closely related. The result of our calculation is shown in Fig. 9 where we conclude that the hydrogen bond symmetrizes at $\sim$450 kbar. This pressure is within the capabilities of the diamond anvil pressure cell method. We also suggest that the vibrational spectrum due to proton dynamics will be considerably different at 450 kbar as compared to the results found at 320 kbar. At the lower pressure, the spectrum still resembled what one expects for perturbed molecular O–H oscillators. However, once the hydrogen bond symmetrizes, the differentiation between covalent and hydrogen bonds no longer applies. Therefore a more appropriate description of the protonic vibrational spectrum is in terms of optical phonons with four distinct branches in the case of ice VII.[5]

Finally, one may question whether the use of a two-state approximation in the pressure regime relevant to the hydrogen-bond symmetrization phenomenon is valid. In this pressure region, the barrier associated with the single bond Morse potential is so small that the energy separation between the lowest two "tunnel split" states is comparable to the energy differences of the higher"vibrational" states. Indeed, the lowest energy state is very close in energy to the barrier height, and once it drifts above the barrier the single bond ground state eigenfunction becomes peaked at the bond center. This suggests an alternative lattice dynamical approach to the hydrogen-bond symmetrization question which we now briefly consider.

In the high pressure, very low barrier regime it is reasonable to replace the double Morse bond potential by an appropriately chosen harmonic oscillator potential. The curvature $k_{\rm eff}$ of the effective harmonic potential is variationally chosen by introducing a trial ground state wave function of the harmonic oscillator form:

$$\Psi_0(r) = (m\omega_0/\pi\hbar)^{1/4}\exp(-m\omega_0 r^2/2\hbar), \tag{3.5}$$

$$k_{\rm eff} \equiv m\omega_0^2, \tag{3.6}$$

where m is the proton mass and ω_0 is a parameter determined by requiring the single bond ground state energy for the true double Morse potential $V_M(r)$ be a minimum when calculated using the trial harmonic oscillator state, i.e.,

$$\frac{\partial}{\partial\omega_0}\left\langle\Psi_0\left|-\frac{\hbar^2}{2m}\frac{d^2}{dr^2}+V_M(r)\right|\Psi_0\right\rangle \equiv 0. \tag{3.7}$$

Equation (3.7) precisely defines $k_{\rm eff} = m\omega_0^2$ for any value of oxygen separation $R_{\rm OO}$. With the effective harmonic oscillator bond potential in hand, we can perform lattice dynamical calculations as described in paper I. For ice VII one obtains a set of eigenfrequencies corresponding to the four optical phonon branches which are labeled by the appropriate reciprocal lattice vectors and are parametric functions of a dimensionless coupling constant[5]

$$\lambda \equiv q^2/a^3 k_{\rm eff}\epsilon_\infty . \tag{3.8}$$

Here a is the unit cell length parameter, q an effective proton charge, and ϵ_∞ the optical dielectric constant. In paper I we showed that as λ was continuously increased (corresponding to continuous decompression of the oxygen lattice), there was a protonic lattice instability signified by the appearance of a soft mode. This instability occurred at a precisely defined value of λ (denoted by λ_c) which was $\simeq$0.08 for ice VII. Since the instability is associated only with the quadratic terms in the proton potential energy, it is natural to interpret it as the lattice dynamical analog of the hydrogen-bond symmetrization point. Therefore the relation

$$\lambda = q^2/\epsilon_\infty a^3 k_{\rm eff}(R_{\rm OO}^{(S)}) \equiv \lambda_c = 0.08 \tag{3.9}$$

represents a closed equation for the oxygen separation $R_{\rm OO}^{(S)}$, where the hydrogen bond symmetrizes. A quantitative implementation of Eq. (3.9) requires the calculation of $k_{\rm eff}(R_{\rm OO})$ via Eq. (3.7), $a = 2R_{\rm OO}/3^{1/2}$ for ice VII, and $q^2/\epsilon_\infty \simeq 0.85e$. (The latter result follows from finite cluster calculations of the singly charged ion formation energy for cubic ice within the context of bond point dipole interactions between protons.[19] The specific value of q^2/ϵ_∞ adopted above follows from requiring that these cluster calculations reproduce the experimental value for ion formation, i.e., 11 kcal/mol.) The result of such a calculation is the prediction of hydrogen-bond symmetrization at $R_{\rm OO} \simeq 2.45$ Å. This is very close to the value of 2.46 Å obtained from the two-state theory. The nearly exact agreement may be fortuitous but the result does give us confidence in our prediction of hydrogen-bond symmetrization in the neighborhood of 450 kbar, using the two-state formalism.

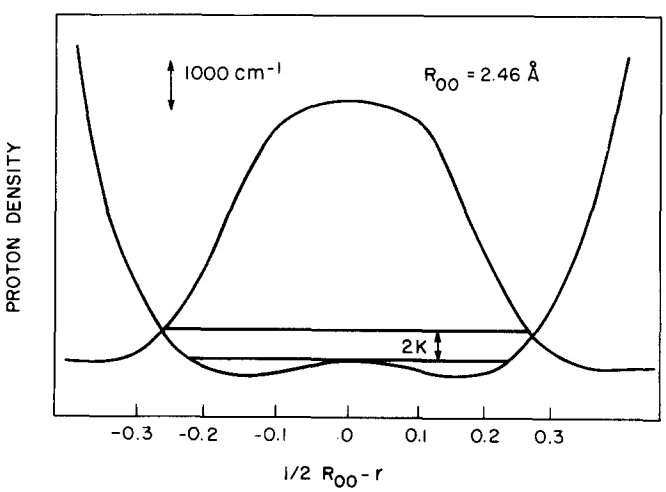

Fig. 9. Proton density in the disordered phase corresponding to the oxygen separation at which the crossover to symmetrical hydrogen bonds occurs. As in Fig. 7 the single bond Morse potential and the tunnel-split energy levels are also displayed.

C. Cubic ice

Our prediction for the pressure needed to form symmetrical hydrogen bonds ($\simeq$450 kbar) in the dense ices is very high but should be attainable with modern experimental

methods. Nevertheless, the experiment will be difficult and it is therefore of interest to consider whether other forms of ice may be better candidates in the search for symmetrical hydrogen bonds. A possibility is cubic ice. While it is known to form only at low pressure it may be possible that if cooled to very low temperature, this form of ice could be compressed to the regime of interest without undergoing oxygen-lattice restructuring (ordinary hexagonal ice should be more susceptible to restructuring). Because of the much lower density of cubic ice compared to the ices VII and VIII, much less pressure should be needed to symmetrize the hydrogen bonds than that required for the dense ices.

With this motivation, we have performed calculations of $\rho(r)$ for cubic ice using the Morse potential parameters in Table I and $\epsilon_1 = 11$ kcal/mol, $\epsilon_2 = 4\epsilon_1$, $J = 0$ (cubic ice is disordered so $x = \frac{1}{2}$ or equivalently $J = 0$). We find that the hydrogen bond symmetrizes at an oxygen separation of $R_{OO} \simeq 2.505$ Å. Equation of state measurements for cubic ice under pressure do not exist. However, because of the structural similarity of cubic and hexagonal ice one expects they will exhibit nearly identical pressure $-R_{OO}$ behavior. For hexagonal ice, the initial pressure derivative is reported to be[17] $\partial R_{OO}/\partial p = 3.8$ Å/Mbar. Also, direct measurement of $R_{OO}(p)$ for the dense ices[2,16] reveals a nearly linear relationship between R_{OO} and pressure up to about 100 kbar. Therefore, if we assume such behavior applies for hexagonal ice, then the above pressure derivative can be used to estimate the pressure needed to compress hexagonal ice (and by implication cubic ice also) from its atmospheric value of $R_{OO} \simeq 2.76$ Å to the point where our calculation predicts hydrogen-bond symmetrization, $R_{OO} \simeq 2.505$ Å. The necessary pressure is found to be 67 kbar. This value is far less than the 450 kbar needed for the dense ices and suggests cubic (or possibly even hexagonal) ice quenched to low temperature may be an easier system to investigate in the search for symmetrically hydrogen-bonded ices.

IV. DISCUSSION

Our prediction for the high pressure phase diagram of ice is shown in Fig. 10. Since we have not performed a finite temperature calculation, the precise nature of the high pressure ice VIII/VII phase boundary is somewhat uncertain. However, we believe the picture presented in Fig. 10 is qualitatively correct, i.e., a nearly horizontal phase boundary between the ordered and disordered dense ices.

The crossover boundary to the symmetrized hydrogen bond regime is indicated by the dashed line. Within the context of our theory, this does not represent a thermodynamic phase change but rather a gradual destruction of short range order. However, one may question whether this conclusion will survive a more exact theoretical analysis. In particular, one can imagine defining a set of $\simeq (3/2)^N$ order parameters corresponding to the full set of canonical neutral water molecule structures. These are nearly degenerate and at finite temperatures contribute entropically to the free energy of the crystal. As the applied pressure is increased, quantum fluctuations will tend to destroy the proton order associated with each neutral state lying low in energy. One can then imagine a "mini" order–disorder transition occurring for

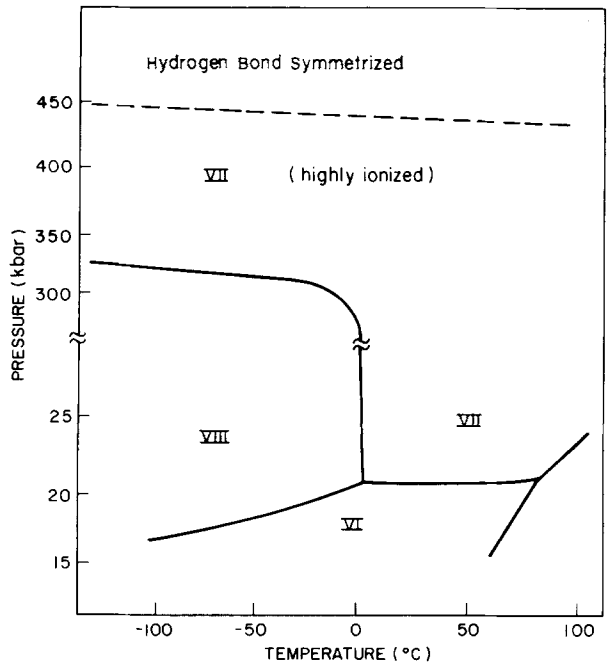

FIG. 10. Predicted high pressure phase diagram for H_2O.

each neutral water molecule state at some specific high pressure. However, because the neutral molecule states do exhibit a small but finite energy dispersion, these symmetry breaking transitions will in principle occur sequentially, i.e., one at a time. One therefore does not expect a macroscopic thermodynamic anomaly to be precipitated by such a phenomenon, and hence the gradual crossover picture should remain valid even for an exact theory.

At pressures not too far above the hydrogen-bond symmetrization point one expects the proton dynamics to be describable in optical phonon terms. The detailed nature of the excitations could be probed via inelastic neutron scattering experiments and the results interpreted with the aid of lattice dynamical calculations such as those performed in paper I.

Finally, we have argued that finite temperature effects due to *classical* fluctuations are probably not important for the very high pressure regime of interest. There remains the question of the nature of the low lying quantum excited states. For three-dimensional magnetic systems which can be described by Heisenberg type spin models, it is well known that there are low lying spin wave excitations. These correspond to small oscillations of the spin direction about the preferred alignment direction. However, for the hydrogen-bonded crystal problem, the proton motion is confined to the linear hydrogen bonds and is therefore of a one-dimensional character. Consequently the analog of an easy axis of magnetization does not seem to exist. One alternative possibility is an excitation spectrum that is particle-like with a finite energy gap separating the ground and first excited states. If the gap is large compared to the thermal energy then our ground state theory should be applicable. Support for this picture is found from the nature of the excitation spectrum of the exactly solvable[20] one-dimensional transverse Ising model. However, a careful study of these questions is needed for the three-dimensional crystals of interest. We are presently studying these matters by attempting to

construct the finite temperature analog of our ground state theory. The fundamental object is the diagonal density matrix (as opposed to the ground state wave function) and the theoretical approach has focused on deriving a closed equation of motion for this function. We hope to return to this aspect in a future publication.

APPENDIX

The purpose of this Appendix is to describe in detail the Morse bond potential and our calculation of the tunnel splitting parameter K. The double Morse bond potential function is defined by

$$V_M(r) = u_M(\tfrac{1}{2}R_{OO} - r_{OH} + r) + u_M(\tfrac{1}{2}R_{OO} - r_{OH} - r) - 2u_M(\tfrac{1}{2}R_{OO} - r_{OH}), \tag{A1}$$

where r is proton distance from the bond midpoint, R_{OO} the oxygen–oxygen separation, r_{OH} the O–H covalent bond length, and the last term in Eq. (A1) simply sets the bond potential energy to zero at the bond midpoint ($r = 0$). The function $u_M(y)$ is the Morse potential:

$$u_M(y) \equiv V_{OH}[1 - \exp(-\alpha_{OH} y)]^2, \tag{A2}$$

and V_{OH} is the sum of the zero point and bond dissociation energies. The corresponding single proton Schrödinger equation is

$$\left[-\frac{\hbar^2}{2m}\frac{d^2}{dr^2} + V_M(r) \right] \Psi(r) = E\Psi(r), \tag{A3}$$

where m is the proton (or deuteron) mass and $\hbar$ is Planck's constant divided by 2π. As discussed in the text we require only the two lowest eigenstates and energies of Eq. (A3). For simplicity, we adopt a variational approach by taking trial wave functions for the lowest two states of the form

$$\Psi_\pm(r) \equiv C_\pm(\sigma_\pm, d_\pm)\{\exp[-\sigma_\pm(r + d_\pm)^2] \pm \exp[-\sigma_\pm(r - d_\pm)^2]\}, \tag{A4}$$

$$C_\pm^2 \equiv \sigma_\pm^{1/2}(2\pi)^{-1/2}[1 \pm \exp(-2\sigma_\pm d_\pm^2)]. \tag{A5}$$

That is, we have chosen as trial states a symmetric and antisymmetric linear combination of displaced Gaussians. By symmetry, these trial states are orthogonal and we can therefore determine the parameters (σ_+, d_+) and (σ_-, d_-) by independent variational energy minimization. Direct calculation of the energy expectation value using the trial wave functions yields

$$\begin{aligned} E(\sigma,d) = (\hbar^2\sigma/2m)\{1 \mp [4\sigma d^2/(\pm 1 + \exp(2\sigma d^2))]\} + \{V_{OH}/[1 \pm \exp(-2\sigma d^2)]\} \\ \times\{[\exp(2\alpha_{OH} d) \pm 2\exp(-2\sigma d^2) + \exp(-2\alpha_{OH} d)] \\ \times\exp\{\alpha_{OH}[\alpha_{OH}(2\sigma)^{-1} + 2r_{OH} - R_{OO}]\} - 2[\exp(\alpha_{OH} d) \pm 2\exp(-2\sigma d^2) + \exp(-\alpha_{OH} d)] \\ \times\exp\{\alpha_{OH}[\alpha_{OH}(8\sigma)^{-1} + r_{OH} - R_{OO}]\}\}, \end{aligned} \tag{A6}$$

where $(\sigma, d) = (\sigma_+, d_+)$ for the ground state and (σ_-, d_-) for the first excited state. Minimization of Eq. (A6) with respect to the two parameters for the two cases yields explicit results for $\sigma_\pm$ and $d_\pm$ as functions of V_{OH}, r_{OH}, R_{OO}, and α_{OH}. From these one can calculate the corresponding energies E_0 and E_1, and thereby compute the tunnel splitting

$$K \equiv (E_1 - E_0)/2. \tag{A7}$$

One also has explicit forms for the ground and first excited state wave functions. In terms of the notation employed in the text:

$$\begin{aligned} \Phi_0(r) &\equiv \Psi_+(r), \\ \Phi_1(r) &\equiv \Psi_-(r). \end{aligned} \tag{A8}$$

Finally, another quantity of importance is the dipole matrix element

$$M_{01} \equiv \langle \Phi_0 | r | \Phi_1 \rangle. \tag{A9}$$

Straightforward manipulations yield the explicit result:

$$\begin{aligned} M_{01} = 2^{1/2}[\sigma_+\sigma_-/(\sigma_+ + \sigma_-)^2]^{1/4}(\sigma_+ + \sigma_-)^{-1}\{[1 + \exp(-2\sigma_+ d_+^2)][1 - \exp(-2\sigma_- d_-^2)]\}^{1/2} \\ \times\{[\sigma_+ d_+ + \sigma_- d_-]\exp[(\sigma_+ d_+ + \sigma_- d_-)^2/(\sigma_+ + \sigma_-)] - [\sigma_+ d_+ - \sigma_- d_-]\exp[(\sigma_+ d_+ - \sigma_- d_-)^2/(\sigma_+ + \sigma_-)]\}. \end{aligned} \tag{A10}$$

[1] A. Jayaraman, Rev. Mod. Phys. **55**, 65 (1983).
[2] G. E. Walrafen, M. Abebe, F. A. Mauer, S. Block, G. J. Piermarini, and R. Munro, J. Chem. Phys. **77**, 2166 (1982).
[3] J. A. Krumhansl and J. R. Schrieffer, Phys. Rev. B **11**, 3535 (1975); A. R. Bishop and J. A. Krumhansl, *ibid.* **12**, 2824 (1975); H. Beck, J. Phys. C **9**, 33 (1976); T. Schneider and E. Stoll, Phys. Rev. B **13**, 1216 (1976); A. D. Bruce and T. Schneider, *ibid.* **16**, 3991 (1977); A. D. Bruce, T. Schneider, and E. Stoll, Phys. Rev. Lett. **43**, 1284 (1979); P. D. Beale, S. Sarker, and J. A. Krumhansl, Phys. Rev. B **24**, 266 (1981).
[4] G. Briganti, V. Mazzacurati, M. A. Ricci, G. Signorelli, and M. Nardone, Solid State Commun. **42**, 493 (1982).
[5] F. H. Stillinger and K. S. Schweizer, J. Phys. Chem. **87**, 4281 (1983).
[6] K. S. Schweizer and F. H. Stillinger, Phys. Rev. B (submitted).
[7] K. S. Schweizer (in preparation).
[8] L. Pauling, J. Am. Chem. Soc. **57**, 2680 (1935); J. D. Bernal and R. H. Fowler, J. Chem. Phys. **1**, 515 (1933).
[9] W. B. Holzapfel, J. Chem. Phys. **56**, 712 (1972).
[10] D. Eisenberg and W. Kauzmann, *The Structure and Properties of Water* (Oxford, New York, 1969).
[11] G. C. Pimentel and A. L. McClellan, *The Hydrogen Bond* (Freeman, San Francisco, 1960), p. 259.
[12] S. Scheiner, J. Am. Chem. Soc. **103**, 315 (1981); J. Phys. Chem. **86**, 376 (1982).
[13] J. C. Slater, J. Chem. Phys. **9**, 16 (1941).
[14] Y. Takagi, J. Phys. Soc. Jpn. **3**, 271 (1948).
[15] M. E. Senko, Phys. Rev. **121**, 1599 (1961).

[16]R. G. Munro, S. Block, F. A. Mauer, and G. Piermarini, J. Appl. Phys. **53**, 6174 (1982).
[17]E. Whalley, in *The Hydrogen Bond. III. Dynamics, Thermodynamics and Special Systems*, edited by P. Schuster, G. Zundel, and C. Sandorfy (North Holland, New York, 1976). But note that G. Johari, J. Phys. Chem. (to be published) claims a substantially larger value.
[18]E. Whalley, D. W. Davidson, and J. B. R. Heath, J. Chem. Phys. **45**, 3976 (1966).
[19]K. S. Schweizer and F. H. Stillinger (unpublished).
[20]P. Pfeuty, Ann. Phys. **57**, 79 (1970).